LASER CLADDING FOR WEAR-RESISTANT COBALT BASE ALLOY AND TUNGSTEN CARBIDE COMPOSITE COATINGS

Yong-Chwang Chen* and Kwo-An Chiang

ABSTRACT

Stellite12 cobalt base alloys with different WC contents were deposited on SK3-carbon tool steel by laser cladding. The behavior of WC particulates, including dissolution and distribution, and the microstructure of WC-Co-Cr-C composite coatings with rapid solidification were investigated. Several significantly different solidified microstructures were characterized by dendrites, eutectics, faceted dendrites and the retained WC particles in the laser cladding WC + Stellite12 coatings, under different laser energy densities. When WC was melted and dissolved into the Stellite12 melt pool, the basic structure of solidification, characterized by the matrix and faceted dendrites in various shapes, and the contents of the faceted dendrites remained nearly identical. The faceted dendrites contained the majority of W as well as some Cr, Co while more Cr and Co were located in the matrix. The X-ray diffraction analyses indicated the existence of σ-Co, $M_{23}C_6$, M_6C and M_7C_3 (M = W, Cr, Co) in the Stellite12 with different WC contents when deposited on substrates by laser cladding. The faceted dendrites provided the coatings with excellent resistance during dry sliding wear test. A higher content of WC gave higher volume fractions of faceted dendrites that imparted excellent wear resistance to the coating.

Key Words: Stellite12, WC, laser cladding, faceted dendrites.

I. INTRODUCTION

Industrial applications of laser surface modification are popular due to the advantages of high power density, thin hardening layer, low heat input and a small heat-affected zone. This is especially true in the application of laser surface cladding for high-technology products. Recently, much attention has been focused on the study of surface cladding of alloys, cements and ceramics. In this process, the laser surface melting followed by rapid self-cooling of the melted layer, can produce very fine microstructures with unusual properties directly on the surface of the work piece (Singh and Mazumder, 1986, 1987; Steen, 1981). In this paper, cobalt-based alloy (Stellite12) and WC-Co-Cr-C composite coatings, produced under different laser energy densities were characterized by scanning electron microscopy (SEM) in order to determine their microstructure evolution. In addition, the wear properties of WC + Stellite12 coatings with rapidly solidified microstructure were investigated.

II. EXPERIMENTAL PROCEDURES

Mixtures of Stellite12 alloy powders and 10%, 20%, and 40% WC powders, respectively, were used as the coating material. The particles of Stellite12 alloy powders were 5 to 10 μm in size. The nominal composition of the Stellite12 alloy powders is listed in Table 1. The particles of the WC powders measured from 5 to 10 μm in size. The high carbon tool steel SK3 (with C > 1.0%) specimen was machined into a rectangular block (30 mm × 8 mm × 8 mm) with a slot (28 mm × 6 mm × 1 mm). Mixtures of Stellite12 alloy powders and WC powders were put into the slot and then treated by laser cladding.

The laser treatment was performed using a 2.0 kW continuous wave CO_2 laser. A Zn-Se lens, with a 190.5 mm focal length was used to focus the beam.

*Corresponding author. (Tel: 886-2-23625489; Fax: 886-2-23625489; Email: d89522007@ntu.edu.tw)

The authors are with the Department of Mechanical Engineering, National Taiwan University, Taipei, Taiwan 106, R.O.C.

Table. 1 Nominal composition of Co-base alloys Stellite12

Wt.%	Co	Cr	C	W	Mo	Ni	Si	B	Fe	Mn
Stellite 12	Bal.	29	1.85	9	-	2.5	1	-	2.5	1

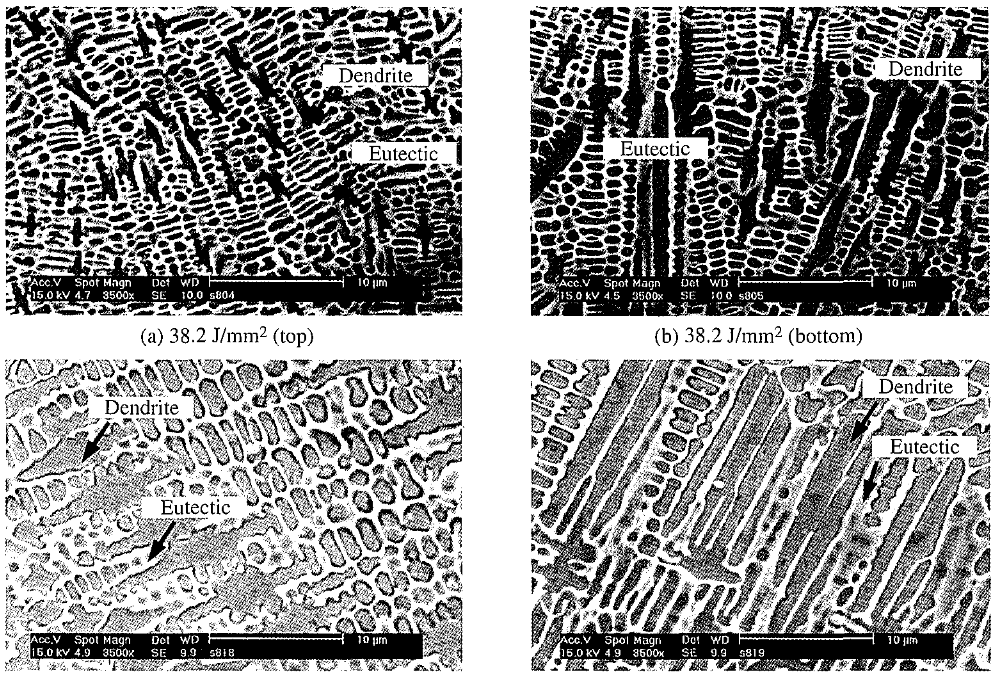

(a) 38.2 J/mm^2 (top)
(b) 38.2 J/mm^2 (bottom)
(c) 66.8 J/mm^2 (top)
(d) 66.8 J/mm^2 (bottom)

Laser energy density	Position	Phase	Co	Cr	W	C	Fe
			Wt.%	Wt.%	Wt.%	Wt.%	Wt.%
38.2 J/mm^2	Top	Eutectic	21.17	35.57	19.59	9.49	14.19
		Dendrite	51.35	25.49	7.34	5.4	10.42
	Bottom	Eutectic	40.78	35.1	13.34	6.92	3.85
		Dendrite	54.31	25.53	11.71	3.41	5.04
66.8 J/mm^2	Top	Eutectic	13.81	34.91	18.33	11.01	21.23
		Dendrite	36.4	16.12	9.61	3.02	34.85
	Bottom	Eutectic	14.01	35.58	18.39	10.19	21.84
		Dendrite	38.68	17.52	8.7	2.21	32.89

(e) Compositional evolution of the dendrites and the eutectics of (a)-(d)

Fig. 1 SEM micrograph and EDX analysis showing the microstructure and compositional evolution of the laser-clad Stellite12 alloy coatings under 38.2 and 66.8 J/mm^2

The laser energy density used in the experiments was in the range 28.65-66.8 J/mm^2, with a 1mm beam diameter. In order to produce oxide free coatings in all experiments, the laser was shielded with N_2 gas. Cross sections of the layers were examined for microstructure and the distribution of hard phases by SEM analysis. The compositions of the clad layers were measured by energy dispersive X-ray (EDX) microanalysis and characterized by X-ray diffraction (XRD).

III. RESULTS AND DISCUSSION

The effects of laser energy density on the microstructure and compositional evolution of the laser-clad Stellite12 alloy layers have been studied using SEM and XRD analyses. Figs. 1(a)-(d) show the cross-section of the laser-clad Stellite12 alloy layers under laser energy density of 38.2 and 66.8 J/mm^2. The typical microstructure of the Stellite12 alloy identified by XRD analysis (as shown in Fig. 2), consists

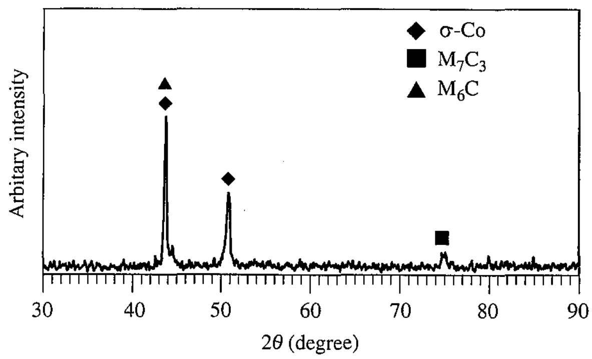

Fig. 2 X-ray diffraction result of the laser-clad Stellite12 coating

of σ-Co (Co-rich matrix) dendrites and eutectics consisting of metallic carbides. According to the Co-Cr-W phase diagram, a Co-rich phase is first formed dendritically from the liquid state. The cooling rate in the liquid state is very high through self-cooling, and Cr and C become enriched in the remaining liquid in the inter-dendrite regions, and then a eutectic carbide structure forms (Nagarathnam and Komvopoulos, 1995; Pizurova *et al.*, 1993; Frenk and Kurz, 1993). The compositional evolutions in the dendrites and eutectics of Fig. 1(a)-(d) by EDX analysis, are listed in Fig. 1(e).

Figures 1(a) and (b) show that the eutectics are much finer at the top of the clad layer than at the bottom. Fig. 1(e) indicates that there are more Cr, W, C and less Co in the eutectics than in the dendrites. The content of Fe in the dendrites and the eutectics is much richer at the top of the clad layer than at the bottom under laser energy density of 38.2 J/mm^2. When we raised the laser energy density from 38.2 J/mm^2 to 66.8 J/mm^2, the eutectics became sparser as revealed by comparing Figs. 1(a) and (b) with Figs. 1(c) and (d). Fig. 1(e) also indicates that the content of Co in the eutectics decreased but the contents of Fe and C in the eutectics increased with increasing laser energy density. At the same time, the contents of Co, Cr and C in the dendrites decreased but the content of Fe increased with increasing laser energy density. It can be seen that when we raised the laser energy density from 38.2 to 66.8 J/mm^2, more Fe from the substrate (SK3 steel) dissolved into the clad layer and formed more metallic carbides in the eutectics.

In Stellite12 alloys, Cr provides oxidation and corrosion resistance as well as strength by the formation of M_7C_3 or $M_{23}C_6$ carbides (M = Co, Cr, W). Refractory metal such as W, which has been known to be a solid-solution hardening element, also contributes to the strength via precipitation hardening by the formation of MC or M_6C carbides, and the intermetallic phase such as Co_3W. In addition, Ni, C and Fe promote the stability of a Co-rich matrix, which is stable at high temperatures up to its melting point of 1495°C.

The effects of the laser energy density on the microstructure and compositional evolution of the laser-clad 10% WC + Stellite12 alloy layers have been studied using SEM analysis. All the SEM microstructure images were taken in the middle part of the laser-clad layers. When 10% WC was added to the Stellite12 alloy powder under laser energy density of 28.65, 38.20, 45.84, 50.93 J/mm^2, respectively, several solidification characteristics were found in the microstructure of the clad layers as shown in Figs. 3 (a)-(d). The first image is characterized by dendrites, eutectics, retained WC particles and fewer faceted dendrites, as shown in Fig. 3(a). The second image is characterized by dendrites and eutectics, retained WC particles and few faceted dendrites as shown in Fig. 3(b). The third one is characterized by dendrites and eutectics, less retained WC particles and faceted dendrites, as shown in Fig. 3(c). The fourth one is characterized by fewer retained WC particles, facet dendrites, dendrites and eutectics, as shown in Fig. 3(d).

In Fig. 3(a), when the laser was removed, the molten Stellite12 started to solidify. The WC particles had hardly melted and dissolved into the Stellite12 melt pool under laser energy density of 28. 65 J/mm^2. When the laser energy density was raised, the added WC particles gradually melted and dissolved into the Stellite12 melt pool. At the same time, more and more faceted dendrites were formed when the laser energy density was increased (Gassmann, 1996). However, some WC particles were still unmelted and the eutectics tended to become dissolved as shown in Figs. 3(b)-(d). When the laser energy density was raised, the extent of the melting of the substrate increased and the clad layers became substantially diluted by Fe, which caused the change of composition and microstructure (Riabkina-Fishman *et al.*, 2001a, 2001b; Yoon *et al.*, 2001). The contents of Co, Cr, W, C and Fe in different solidification characteristics of Figs. 3 (a)-(d), as determined by EDX analysis, are listed in Fig. 3(e). Dilution rate is calculated as the percentage of the mixture area to the entire transverse clad area. Fig. 3(e) indicates that the dilution rate increased gradually when we raised the laser energy density. This is because a larger area of substrate was melted when we raised the laser energy, thus more energy of the laser beam was absorbed by the substrate.

When the laser energy density was raised, the contents of Cr, W and C in eutectics decreased gradually. At the same time, the content of Co in eutectics increased. It is seen that the Cr, W and C in eutectics tend to dissolve into the facet dendrites and Co tends to dissolve into the dendrites. EDX analysis from Fig.

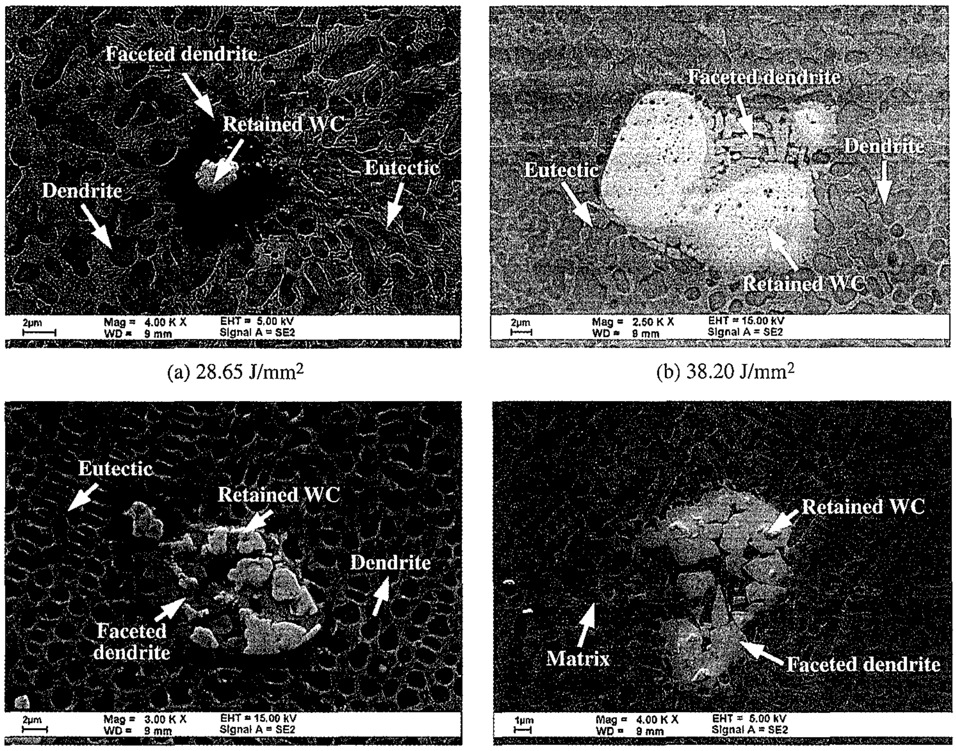

(a) 28.65 J/mm^2 (b) 38.20 J/mm^2

(c) 45.84 J/mm^2 (d) 50.93 J/mm^2

Laser energy density	Dilution rate (%)		Co	Cr	W	C	Fe
			Wt.%	Wt.%	Wt.%	Wt.%	Wt.%
28.65 J/mm^2	8.1	Retained WC	0	0	93.09	6.91	0
		Dendrite	60.89	21.46	12.87	0	4.79
		Eutectic	26.60	35.6	29.47	5.50	2.83
38.20 J/mm^2	10.1	Retained WC	0	0	96.87	3.13	0
		Faceted dendrites	21.16	13.76	61.54	2.36	1.18
		Dendrite	52.83	27.84	14.45	0	4.88
		Eutectic	33.98	31.68	27.14	5.2	2.00
45.84 J/mm^2	10.6	Retained WC	0	0	91.6	8.4	0
		Faceted dendrites	16.69	8.67	70.13	4.52	0
		Dendrite	48.82	30.64	15.54	0	5
		Eutectic	36.14	30.83	25.07	4.63	3.33
50.93 J/mm^2	11.3	Retained WC	0	0	95.84	4.16	0
		Faceted dendrites	17.38	8.02	71.68	2.08	0.85
		Matrix	20.52	31.9	14.61	4.25	28.72

(e) Compositional evolution of the retained WC, faceted dendrites, dendrites, eutectics and the matrix of (a)-(d)

Fig. 3 SEM micrograph and EDX analysis showing the microstructure and the compositional evolution of the laser-clad 10%WC + Stellite12 coatings; (a) 28.65 J/mm^2 (b) 38.20 J/mm^2 (c) 45.84 J/mm^2 (d) 50.93 J/mm^2

3(e) indicates that there is less Co, Cr and C in the facet dendrites compared to the eutectic, but there is more W than in the eutectics and the dendrites. The content of Co in the dendrites decreased but the content of Fe increased because more Fe from the substrate (SK3 steel) dissolved into the clad layer when we raised the laser energy density. When more WC was added, it was evident that more faceted dendrites appeared as shown in Fig. 4. At the same time, more un-melted WC was found in the clad layer when we raised the WC content from 20% to 40%.

Figure 5(a) shows that, when carefully observed,

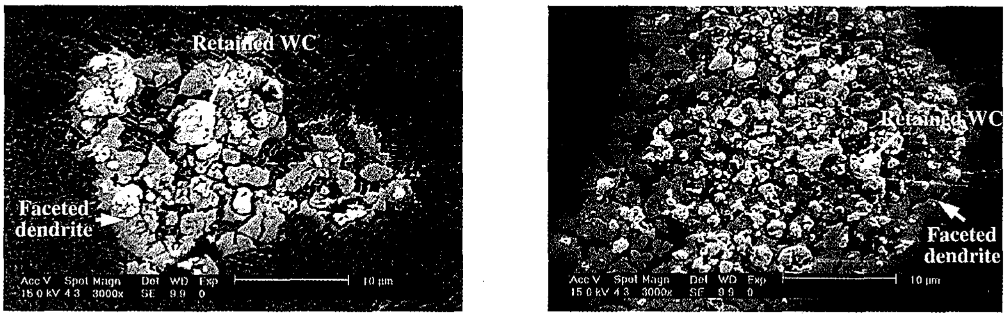

(a) 20%WC + Stellite12 alloy coating (b) 40%WC + Stellite12 alloy coating

Fig. 4 SEM micrograph showing the microstructure of the laser-clad (a) 20%WC + Stellite12 coating, (b) 40%WC + Stellite12 alloy coating under 45.84 J/mm^2 laser energy density

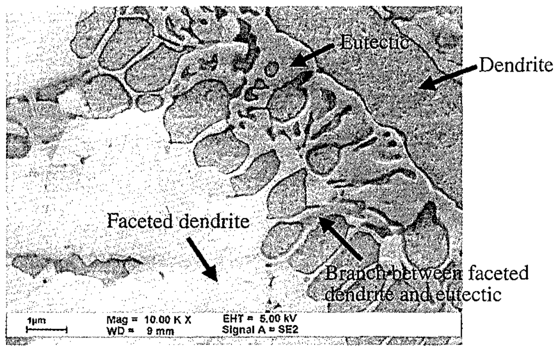

(a) SEM micrograph of the laser clad 10%WC + Stellite12 alloy coating

Laser energy density		Co Wt.%	Cr Wt.%	W Wt.%	C Wt.%
38.20 J/mm^2	Faceted dendrites	13.25	5.94	65.56	15.25
	Branch between faceted dendrites and eutectic	21.61	19.48	43.48	15.43
	Eutectic	27.88	32.98	18.97	20.16
	Dendrite	53.1	19.88	11.19	15.83

(b) Compositional evolution in the faceted dendrites, branch between faceted dendrites and eutectic, dendrites and the eutectics of (a)

Fig. 5 SEM micrograph and EDX analysis showing the microstructure and the compositional evolution of the laser-clad 10%WC + Stellite12 coating under 38.20 J/mm^2 laser energy density

it can be seen that this faceted dendrite appears in the eutectic carbides. EDX analysis as shown in Fig. 5(b) indicates that the contents of Co, Cr, and C in eutectic carbides seem to diffuse into the faceted dendrite. It was noted earlier that the basic microstructure of the laser-clad of Stellite12 is σ-Co (Co-rich matrix) dendrite and eutectics consisting of metallic carbides. Some alloying elements, like W, extend into the dendrites, and most of the W is contained in the eutectics. However, when more W enters into the melt, neither the eutectic nor the dendrite is able to contain the large amount of W. Consequently the remaining W presumably solidifies into a faceted dendrite structure in some form of tungsten carbides which contain more W. Since most of the W is contained in the eutectics, the redundant W can only solidify in the eutectic area (Zhong *et al.*, 2002).

The effects of the different WC additions on the microstructure and compositional evolution of the laser-clad WC + Stellite12 alloy layers have been studied using SEM analysis. SEM micrographs of cross-sections of the 10%, 20%, and 40%WC + Stellite12 alloys coating under laser energy density of 66.8 J/mm^2 are shown in Figs. 6(a)-(c). It is evident that the more WC was added, more was dissolved into the Stellite12 melt pool. The basic solidification characterized by the retained WC, matrix and faceted dendrites in various shapes of the clad layers

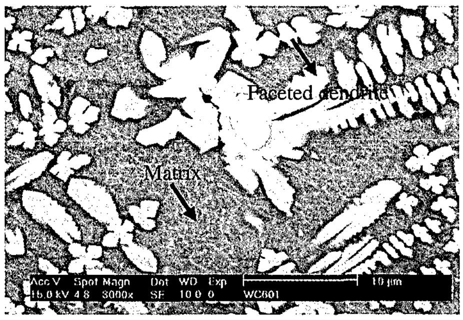

(a) 10%WC + Stellite12 alloys

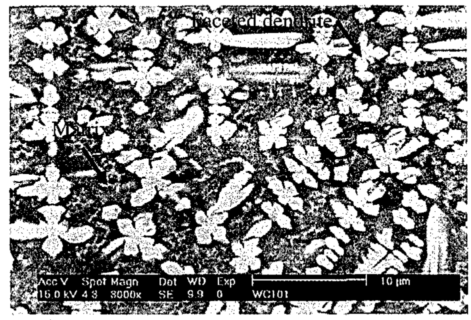

(c) 20%WC + Stellite12 alloys

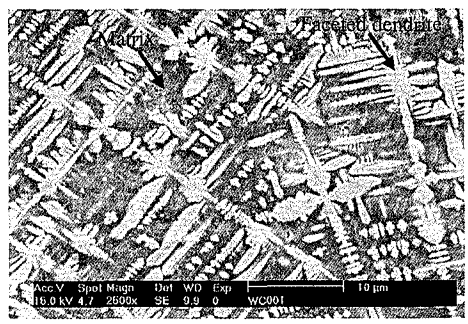

(c) 40%WC + Stellite12 alloys

Contents	Dilution rate (%)		Co	Cr	W	C	Fe
			Wt.%	Wt.%	Wt.%	Wt.%	Wt.%
10%WC + Stellite12	11.5	Faceted dendrites	16.21	11.0	67.71	2.21	2.87
		Matrix	45.95	25.38	19.20	4.74	4.73
20%WC + Stellite12	12.1	Faceted dendrites	18.7	12.89	63.72	2.39	2.3
		Matrix	46.92	26.49	18.21	3.56	4.82
40%WC + Stellite12	15.4	Faceted dendrites	18.14	10.04	66.54	2.14	3.14
		Matrix	44.65	25.93	17.79	1.78	9.85

(d) Compositional evolution in the faceted dendrites and the matrix of the WC + Stellite12 alloys coating under 66.8 J/mm^2 laser energy density

Fig. 6 SEM micrograph of cross-section of the (a) 10%WC+ Stellite12 (b) 20%WC + Stellite12 (c) 40%WC + Stellite12 coatings under 66.8 J/mm^2 laser energy density, (d) compositional evolution in the faceted dendrites and the matrix of the WC + Stellite12 coatings

were maintained in almost identical form. When we added more WC from 10% to 40%, the volume of the facet dendrites increased. In Fig. 6(d), when the added WC increases, the dilution rate also increases. This is due to the low heat capacity of WC, thus more energy of the laser beam was absorbed by the substrate when we raised the content of WC. However, the contents of Cr, W and C in faceted dendrites were almost identical. Fig. 6(d) also shows that due to the melting of the substrate and the dilution of the clad layers, the matrix contained more and more Fe.

Backscattered electron images and elemental mappings of the 40% WC + Stellite12 coating under laser energy density of 66.8 J/mm^2 are shown in Figs. 7(a)-(d). It is worth noting that the distribution of W becomes noticeably concentrated in the faceted dendrites, while Cr and Co are mostly located in the matrix.

X-ray diffraction analyses (Fig. 8) indicate the existence of σ-Co(Co-rich matrix phase), $M_{23}C_6$ type carbides with an f. c. c crystal structure , M_6C and M_7C_3 with orthorhombic crystal structures (M = W, Cr, Co) in the 10% and 20%WC+Stellite12 alloy coatings receiving laser energy density of 50.93 J/mm^2 (Wu *et al.*, 1995). It is not easy to identify the carbides through a simple comparison of XRD peaks and JCPDS values because of the wide range of solubility limits of most carbides. By comparing the X-ray diffraction patterns of 10%, 20% and 40%WC + Stellite12 alloy coatings, it was noticed that the carbides transformed from M_7C_3 to $M_{23}C_6$ when the content of WC reached 40%.

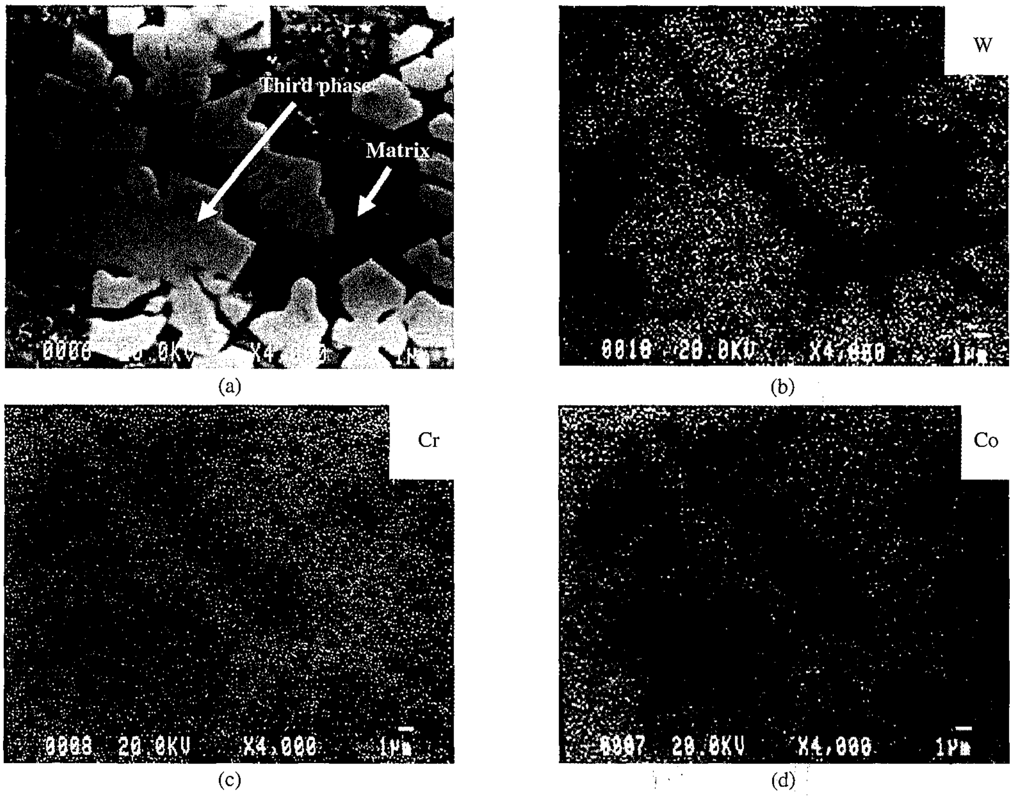

Fig. 7 Backscattered electron images and elemental mapping of cross-section of the 40%WC+ Stellite12 coating under 66.8 J/mm^2 laser energy density; (a) Backscattered electron image, (b) W element distribution, (c) Cr element distribution, (d) Co element distribution

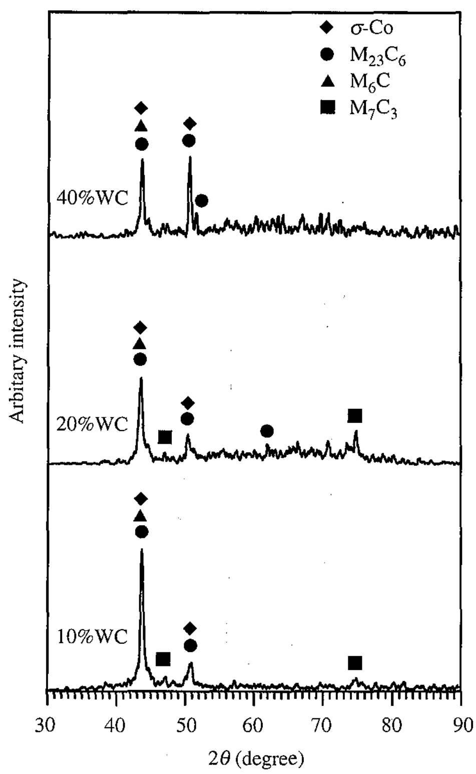

Fig. 8 X-ray diffraction result of the laser-clad 10, 20, and 40%WC + Stellite12 coatings

The laser cladding of Stellite12 cobalt base alloys with WC composite coatings exhibits excellent wear resisting properties under pin on disk dry sliding wear test conditions, as shown in Fig. 9. It is clearly indicated that the Stellite12 cobalt base alloys with 10% and 20% WC content composite coatings are much more wear-resistant than the laser-clad Stellite12 cobalt base alloy coatings itself and the quenched-tempered SK3 steels when tested under the wear test conditions of 0.146 Mpa and 0.049 Mpa loading and a sliding speed of 0.226 m/s for 10.053 km.

The significant improvements of wear resistance of the laser cladding of WC + Stellite12 coatings could be attributed to the faceted dendrites. When we compare the contact surface of laser-clad 10% WC + Stellite12 composite coating and Stellite12 coating itself before and after wear test by SEM as shown in Fig. 10, we find that there are some outstanding particles on the contact surface of the laser-clad 10% WC + Stellite12 coatings. Fig. 11 shows that, when carefully observed, it is evident that these outstanding particles on the contact surface exhibit higher wear resistance than the matrix. EDX analysis also indicates that the contents of W, Co, Cr, Fe and C in these outstanding particles are similar to those in the faceted dendrite. The faced dendrites provide the

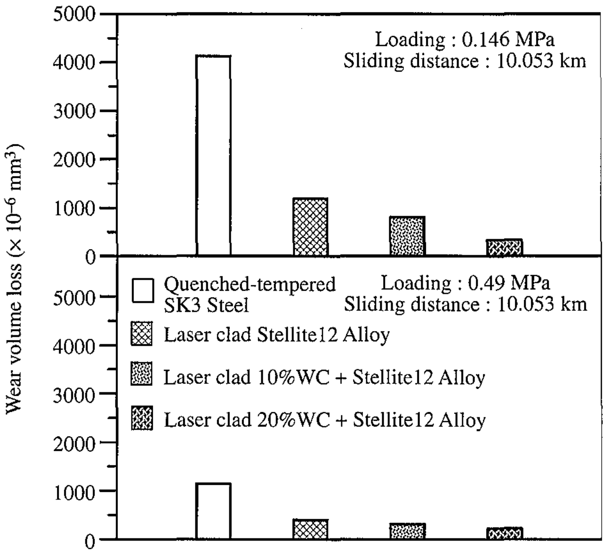

Fig. 9 Comparison of the wear volume loss under pin on SKD61 disk dry sliding wear test conditions

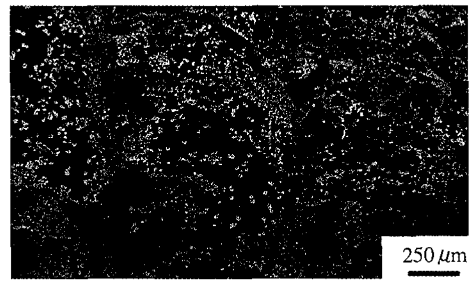

(a) Stellite12 coating (before wear test)

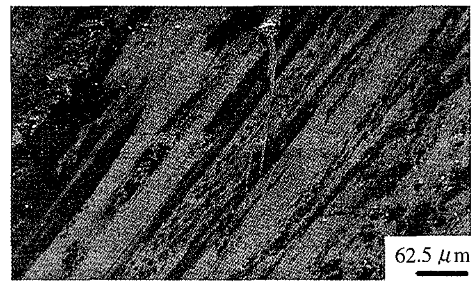

(b) Stellite12 coating (after wear test)

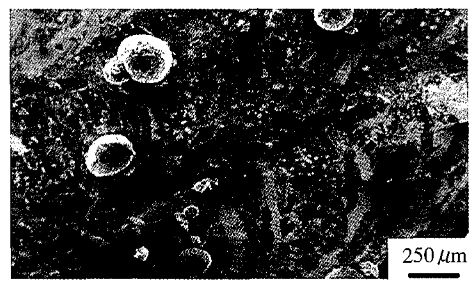

(c) 10%WC + Stellite12 coating (before wear test)

(d) 10%WC + Stellite12 coating (after wear test)

Fig. 10 SEM micrograph showing the contact surface of the laser-clad Stellite12 and 10%WC + Stellite12 coatings under 50.93 J/mm^2 laser energy density before and after the wear test

coatings with excellent resistance to metallic adhesion during dry sliding wear test. The higher content of WC gives higher volume fractions of faceted dendrites that prevent the Stellite12 cobalt base alloys with WC composite coatings from wear attacks of micro-cutting and plowing. In other words, it is the existence of a high volume fraction of the wear-resistant faceted dendrites in the Stellite12 cobalt base alloys with WC composite coatings that imparts excellent wear resistance.

IV. CONCLUSIONS

Several significantly different solidification characteristics are found in the laser cladding WC + Stellite12 alloy coatings. When the laser energy density is raised, the added WC particles gradually melt and dissolve into the Stellite12 melt pool. At the same time, more and more faceted dendrites are formed when the laser energy density increases. EDX analysis indicates that there is less Co, Cr and C in this faceted dendrite compared to the eutectic, and the main characteristic is that the faceted dendrite carries more than 60 (wt%)W, which is substantially higher than the W content in either the eutectic matrix itself or the dendrites. When we raised the addition of WC, more WC is melted and dissolved into the Stellite12 melt pool, the basic structure of solidification, characterized by the matrix and faceted dendrites in various shapes, and the compositional evolution of the clad layers remain nearly identical. The faceted dendrites contain the majority of W as well as some Cr and Co, while there are more Cr and Co located in the matrix. The X-ray diffraction analyses indicate the existence of σ-Co, $M_{23}C_6$, M_6C and M_7C_3 (M = W, Cr, Co) in the 10% and 20%WC + Stellite12 alloy coatings. It is noticed that the carbides transform from M_7C_3 to $M_{23}C_6$ when 40% WC is added to the Stellite12 powder. The faceted dendrites provide the coatings with excellent resistance to metallic adhesion during dry sliding wear test. The higher content of WC gives higher volume fractions of faceted dendrites that impart excellent wear resistance to the coating.

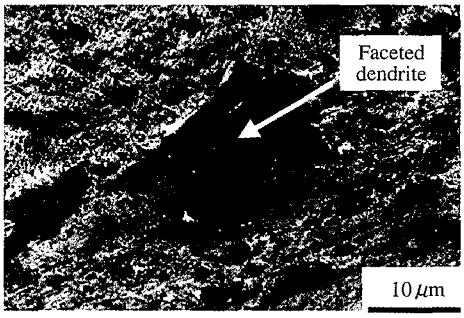

(a) Contact surface before were test

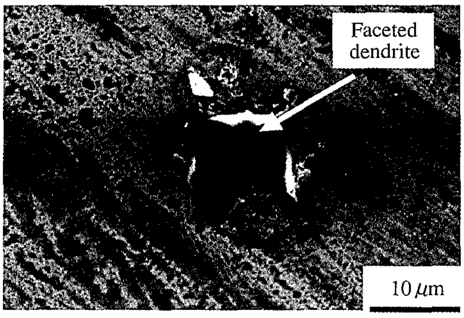

(b) Contact surface after were test
(Laoding : 0.146 Mpa, Sliding distance : 10.053 km)

Fig. 11 SEM micrograph showing the contact surface of the laser-clad 10%WC + Stellite12 coating under 50.93 J/mm^2 laser energy density before and after the wear test

REFERENCES

Frenk, A., and Kurz, W., 1993, "High Speed Laser Cladding: Solidification Conditions and Microstructure of a Cobalt-Based Alloy," *Materials Science & Engineering A*, Vol. 173A, pp. 339-342.

Gassmann, R. C., 1996, "Laser Cladding with (WC + W_2C)/Co-Cr-C and (WC + W_2C)/Ni-B-Si Composites for Enhanced Abrasive Wear Resistance, " *Materials Science and Technology*, Vol. 12, No. 8, pp. 691.

Nagarathnam, K., and Komvopoulos, K., 1995, "Microstructural and Microhardness Characteristics of Laser-Synthesized Fe-Cr-W-C Coatings," *Metallurgical and Materials Transactions A*, Vol. 26A, No. 8, pp. 2131-2139.

Pizurova, N., Komurka, J., Svoboda, M., and Schneeweiss, O., 1993, "Structure and Phase Composition of Cobalt Rich Coating Prepared by Laser Cladding on Low Carbon Steel," *Materials Science and Technology*, Vol. 9, No. 2, pp. 172-175.

Riabkina-Fishman, M., Rabkin, E., Levin, P., Frage, N., Weisheit, A., Galun, R., and Mordike, B. L., 2001a, "Laser Produced Functionally Graded Tungsten Carbide Coatings on M_2 High-Speed Tool Steel" *Materials Science and Engineering A*, Vol. 302, No. 1, pp. 106-114.

Riabkina-Fishman, M., Rabkin, E., Galun, R., Maiwald, T., and Mordike, B. L., 2001b, "Structure and Composition of Laser Produced WC Alloyed Layers on M_2 High-Speed Steel," *Journal of Materials Science Letters*, Vol. 20, No. 20, pp. 1917-1920.

Singh, J., and Mazumder, J., 1986, "Evolution of Microstructure in Laser Clad Fe-Cr-Mn-C Alloy," *Materials Science and Technology*, Vol. 2, No. 7, pp. 709-713.

Singh, J., and Mazumder, J., 1987, "Microstructure and Wear Properties of Laser Clad Fe-Cr-Mn-C Alloy," *Metallurgical Transactions A*, Vol. 18A, pp. 313-322.

Steen, W. M., and Powell, J., 1981, "Laser Surface Treatment," *Materials in Engineering*, Vol. 2, No. 3, pp. 157-162.

Wu, P., Zhou, C. Z., and Tang, X. N., 1995, "Laser Alloying of a Gradient Metal-Ceramic Layer to Enhance Wear Properties," *Surface and Coatings Technology*, Vol. 73, pp. 111-114.

Yoon, J. S., Lee, H.Y., Han, J. G., Yang, S. H., and Musil, J., 2001, "The Effect of Al Composition on the Microstructure and Mechanical Properties of WC-TiAlN Superhard Composite Coating," *Surface and Coatings Technology*, Vol. 142-144, pp. 596-602.

Zhong, Minlin, Liu, Wenjin, Yao, Kefu, Goussain, Jean-Claude, Mayer, Cécile, and Becker, Ahim, 2002, "Microstructural Evolution in High Power Laser Cladding of Stellite 6 + WC Layers," *Surface and Coatings Technology*, Vol. 157, pp. 128-137.

Manuscript Received: Oct. 06, 2004
Revision Received: Apr. 20, 2005
and Accepted: May 25, 2005